



Synthesis and biological evaluation of *N*-alkyl-*N*-(4-methoxyphenyl)pyridin-2-amines as a new class of tubulin polymerization inhibitors

Xiao-Feng Wang^a, Emika Ohkoshi^b, Sheng-Biao Wang^a, Ernest Hamel^c, Kenneth F. Bastow^d, Susan L. Morris-Natschke^b, Kuo-Hsiung Lee^{b,e}, Lan Xie^{a,*}

^a Beijing Institute of Pharmacology and Toxicology, 27 Tai-Ping Road, Beijing 100850, PR China

^b Natural Products Research Laboratories, UNC Eshelman School of Pharmacy, University of North Carolina at Chapel Hill, NC 27599, USA

^c Screening Technologies Branch, Development Therapeutics Program, Division of Cancer Treatment and Diagnosis, National Cancer Institute at Frederick, National Institute of Health, Frederick, MD 21702, USA

^d Division of Chemical Biology and Medicinal Chemistry, UNC Eshelman School of Pharmacy, University of North Carolina at Chapel Hill, NC 27599, USA

^e Chinese Medicine Research and Development Center, China Medical University and Hospital, Taichung, Taiwan

ARTICLE INFO

Article history:

Received 18 September 2012

Revised 21 November 2012

Accepted 29 November 2012

Available online 6 December 2012

Keywords:

N-Alkyl-*N*-phenylpyridin-2-amines

Cytotoxicity

Tubulin polymerization inhibitors

Colchicine binding site

ABSTRACT

Based on our prior antitumor hits, 32 novel *N*-alkyl-*N*-substituted phenylpyridin-2-amine derivatives were designed, synthesized and evaluated for cytotoxic activity against A549, KB, KB_{VIN}, and DU145 human tumor cell lines (HTCL). Subsequently, three new leads (**6a**, **7g**, and **8c**) with submicromolar GI₅₀ values of 0.19–0.41 μM in the cellular assays were discovered, and these compounds also significantly inhibited tubulin assembly (IC₅₀ 1.4–1.7 μM) and competitively inhibited colchicine binding to tubulin with effects similar to those of the clinical candidate CA-4 in the same assays. These promising results indicate that these tertiary diarylamine derivatives represent a novel class of tubulin polymerization inhibitors targeting the colchicine binding site and showing significant anti-proliferative activity.

© 2012 Elsevier Ltd. All rights reserved.

1. Introduction

Microtubules are formed by polymerization of heterodimers of α - and β -tubulin, and play important roles in cellular activities, including cell structure maintenance, intracellular transport, mitosis, and cell division. Taxoids and vincristine alkaloids are two well-known classes of anticancer drugs that act as tubulin inhibitors by targeting two distinct binding sites (i.e., taxol and vinca sites) on the α , β -tubulin heterodimer^{1,2} and disrupting the dynamics of microtubule assembly and disassembly. They are effective in the clinical treatment of cancers, but do have certain deficiencies, including narrow therapeutic indexes and emergence of drug resistance. In efforts to overcome these drawbacks, many new tubulin inhibitors, which are targeted at the colchicine site, a third distinct binding site on tubulin, have been discovered recently and are the subjects of intense investigation. Figure 1 shows examples of such inhibitors, including plant natural products and derivatives, as well as synthetic small molecules. Because of their synthetic accessibility and structural diversity, certain small molecule drug candidates, such as CA-4, ABT-751, and MPC-6827, are currently undergoing clinical trials for treating cancers. These results greatly

encourage further efforts to design and discover novel small molecules that function as tubulin polymerization inhibitors targeted at the colchicine binding site.

In our prior studies, we discovered two synthetic hits 6-chloro-*N*-(4-methoxyphenyl)-3-nitropyridin-2-amine (**1a**) and 6-chloro-2-(4-methoxyphenoxy)-3-nitropyridine (**1b**) by using cell assay screening. They showed promising cytotoxic activity (GI₅₀ values 2.40–13.5 μM and 1.18–2.03 μM, respectively) against a panel of human tumor cell lines (HTCL), including A549, KB, KB_{VIN}, and DU145.³ While the only structural difference between **1a** and **1b** is the linker (NH or O) between the two aryl rings (A and B rings), **1b** was two- to seven-fold more potent than **1a**. Therefore, we postulated that the linker might be associated with the molecular antitumor potency. By performing a conformation analysis using a molecular mechanics (MM2) method with energy minimization and dynamics calculation,⁴ we found that the phenyl and pyridine rings of compounds **1a** and **1b** have quite different spatial orientations as shown in Figure 2. Compound **1a** has a conjugated resonance system and a planar conformation, in which an intramolecular hydrogen bond between the hydrogen of the NH linker and an oxygen atom of the *ortho*-nitrogen group orients the phenyl and pyridine rings (A and B rings) in the same plane. The presence of the intramolecular H-bond was validated by a down-field signal (δ 10.17 ppm) for the NH proton in the ¹H

* Corresponding author. Tel./fax: +86 10 6931690.

E-mail address: lanxieshi@yahoo.com (L. Xie).

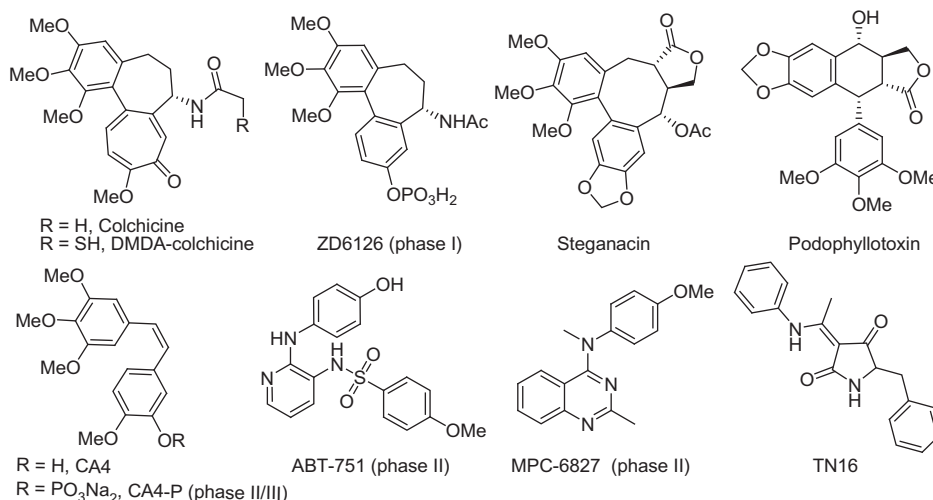


Figure 1. Plant natural products, derivatives, and synthetic compounds as tubulin inhibitors targeted at the colchicine binding site. Some of them are in clinical trials.

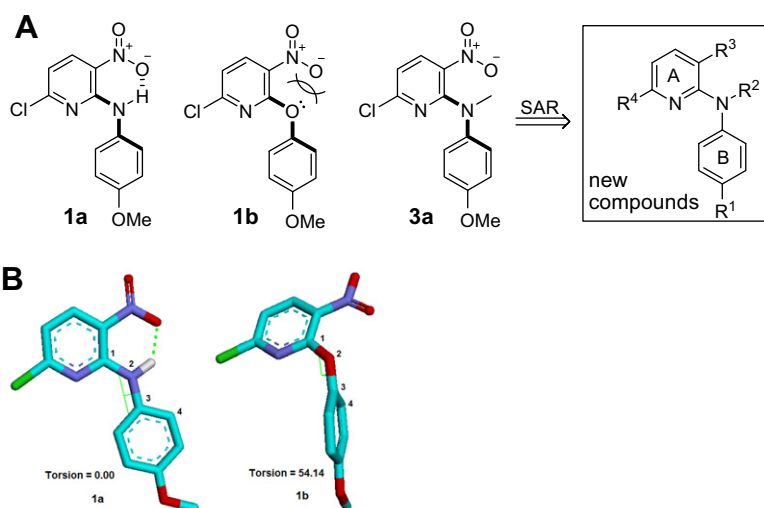


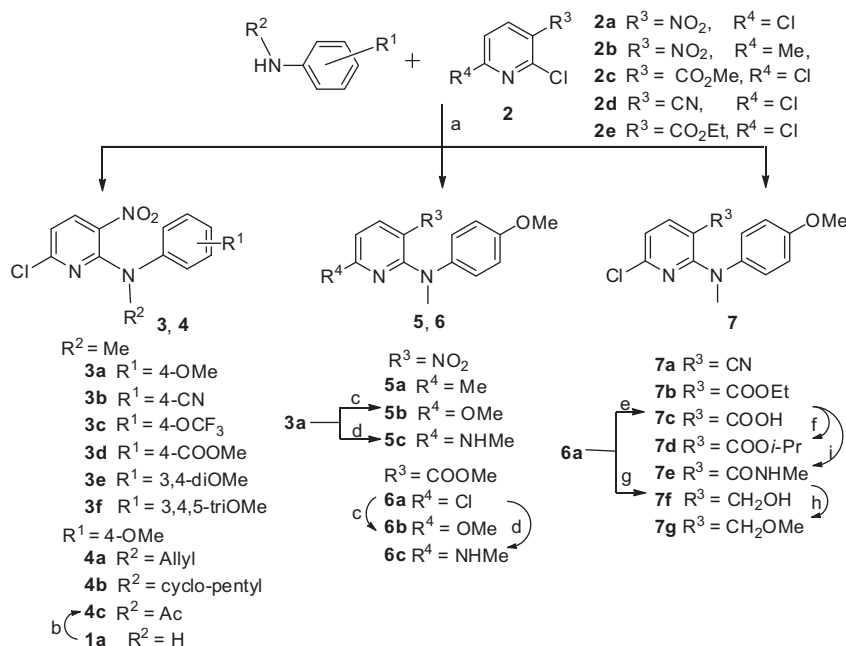
Figure 2. (A) Hits, design, and a general formula of new tertiary diarylamines. (B) Preferred conformations of **1a** and **1b**. The torsional angle C1–N2–C3–C4 is defined as positive if, when viewed along the N2–C3 bond, atom C1 must be rotated clockwise to eclipse atom C4.

NMR spectrum of **1a**. In contrast, the conformation of **1b** shows a torsional angle of 54.14° [C1–N2–C3–C4] between the two aryl rings, caused by electronic repulsion between lone-pair electrons of the linker oxygen and the negatively charged *ortho*-nitro group. Therefore, we hypothesize that a non-planar molecular conformation might be favorable for enhancing antitumor potency. Even though **1a** is less active than **1b**, the NH linker of **1a** is modifiable and steric hindrance can be introduced to promote a non-planar molecular conformation. Consequently, 6-chloro-*N*-(4-methoxyphenyl)-*N*-methyl-3-nitropyridin-2-amine (**3a**), a tertiary amine derivative of **1a**, was designed and synthesized. In another positive design direction, **3a** contains a 4-methoxy-*N*-methylanilino moiety as also found in MPC-6827. Compound **3a** exhibited significant cytotoxic activity against a panel of human tumor cell lines with low micromolar GI₅₀ values of 1.55–2.20 μM. Accordingly, additional tertiary diarylamine derivatives **3–8** were designed, synthesized, and evaluated for antitumor activity. The new target compounds are shown in the general formula in Figure 2. The impact of substituents [R¹ on the B-ring, R² on the linker (Y), R³ and R⁴ on the A-ring] on the cytotoxic activity was investigated successively. Furthermore, new active leads with high potency were tested in anti-tubulin assays to identify a potential biological target

and possible binding site. Our new results on the tertiary diarylamines, including chemical synthesis, cytotoxicity against human tumor cells, SAR results, and identification of biological target, are presented herein.

2. Chemistry

As shown in Scheme 1, the designed target compounds **3–7** could be synthesized from substituted 2-chloropyridines (**2**) and various commercially available anilines. Most of the compounds were prepared by a coupling reaction between **2** and a substituted aniline in *t*-BuOH in the presence of potassium carbonate either at room temperature for 12–24 h⁵ (method A for **3a**, **3e**, **3f**) or under microwave irradiation at 120–160 °C for 10–30 min (method B for **3c**, **3d**).^{6,7} As an exception, the coupling of 2,6-dichloro-3-nitropyridine (**2a**) with *N*-methyl 4-cyanoaniline was carried out by direct heating under solvent-free conditions to provide **3b** in 37% yield. Consistent with our previous results,⁸ the nucleophilic *N*-substituted aniline preferred to attack the 2,6-dichloropyridine (**2**) at the 2-chloro position, which is *ortho* to an electron-withdrawing substituent R³ (such as NO₂, COOMe, and COOEt in **2a**, **2c**, and **2e**, respectively) to produce corresponding series **3–7**



Scheme 1. Synthesis of **3–7** series. (a) neat, 140 °C, N₂, 4 h for **3b**; K₂CO₃/*t*-BuOH, rt, 12–24 h or microwave irradiation, 120–160 °C, 10–30 min for others; (b) Ac₂O/H₂SO₄, 90 °C, 18 h; (c) NaOMe/MeOH, reflux, 2 h; (d) MeNH₂/MeOH, reflux, 12 h; (e) (i) aq NaOH (3 N), THF/MeOH, rt, 36 h; (ii) HCl (2 N); (f) *i*-PrI, K₂CO₃, acetone, reflux, 4 h; (g) LiBH₄, THF, MeOH, rt, 2 h; (h) CH₃I, NaH (60% oil suspension), THF, rt, 2 h; (i) (i) HOBT, EDCI, CH₂Cl₂, rt, 30 min; (ii) NH₂Me (30% in MeOH), 1.5 h, rt.

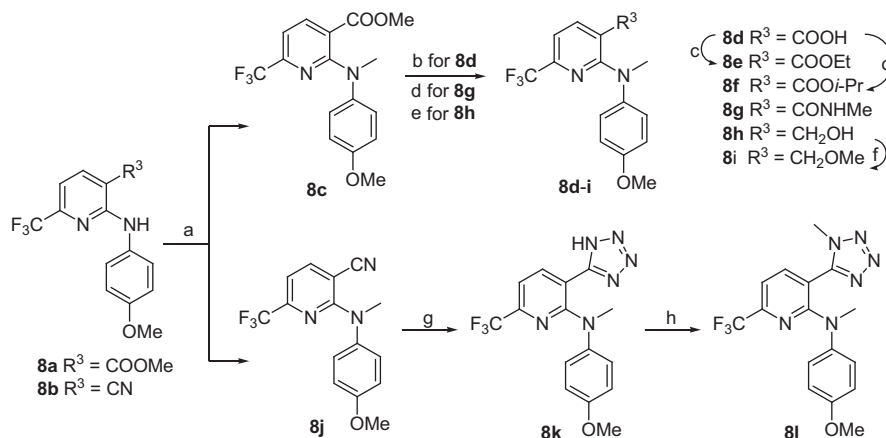
compounds. However, when 3-cyano-2,6-dichloropyridine (**2d**) was treated with *N*-methyl-4-methoxyaniline, 2- (**7a**) and 6-anilino products were formed in a 1:2 ratio, indicating that the presence of the cyano (CN), a weak electron-withdrawing group, led to less selectivity between the two chlorinated *ortho*- and *para*-positions on the pyridine ring. By using the same aromatic nucleophilic substitution reaction, compounds **4a**, **4b**, **5a**, **6a**, **7a**, and **7b** were prepared from the appropriate chloropyridines **2a–e** and *N*-substituted 4-methoxyanilines. Acetylation of hit **1a** with acetic anhydride in the presence of a catalytic amount of concentrated sulfuric acid provided compound **4c**. The 6-chloro in **3a** and **6a** was converted to a methoxy or methylamine group by treatment with sodium methoxide or methylamine in dry MeOH to produce corresponding compounds **5b**, **6b** or **5c**, **6c**, respectively. Hydrolysis of **6a** under basic conditions gave the carboxylic acid compound **7c**, which was esterified with 2-iodopropane in acetone to produce **7d**. The treatment of **7c** with 1-hydroxybenzotriazole (HOBt) in the presence of 1-ethyl-3-(3-dimethylaminopropyl) carbodiimide (EDCI) hydrochloride salt, followed by the reaction with methylamine (30% in MeOH) gave **7e**, with 3-CONHMe (R^3) on the pyridine ring, in moderate yield.⁹ Additionally, the ester group in **6a** was reduced by reaction with lithium borohydride (LiBH₄) to give 3-hydroxymethyl compound **7f**, which was converted to 3-methoxymethyl compound **7g** by treatment with iodomethane in the presence of sodium hydride in anhydrous DMF.

Scheme 2 shows the synthesis of 6-trifluoromethylpyridine compounds **8c–l** from 3-substituted *N*-(4-methoxyphenyl)-6-trifluoromethylpyridin-2-amine **8a** ($R^3 = COOMe$) or **8b** ($R^3 = CN$), which were prepared by literature methods.¹⁰ Methylation of **8a** and **8b** with methyl iodide in the presence of sodium hydride in DMF at low temperature (0 °C) produced tertiary amines **8c** and **8j**, respectively. Hydrolysis, aminolysis, or reduction of the ester group in **8c** produced corresponding benzoic acid (**8d**), *N*-methyl carboxamide (**8g**), and hydroxymethyl (**8h**) compounds, respectively. Further esterification of **8d** with iodoethane or 2-iodopropane in refluxing acetone gave ethyl ester **8e** and isopropyl ester

8f, respectively. Similarly to the preparation of **7g**, methylation of **8h** afforded methoxymethyl compound **8i**. A tetrazolyl ring (R^3) was formed¹¹ from the cyano group in **8j** by treatment with sodium azide and triethylamine hydrochloride in refluxing toluene to afford **8k**. However, this reaction did not go to completion, and ca. one-third of the starting **8j** was recovered, even after 36 h. Furthermore, methylation of **8k** with dimethyl sulfate produced the corresponding **8l**. All target compounds were identified by ¹H NMR and MS spectroscopic data, and purity was determined by HPLC.

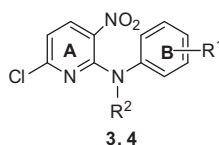
3. Results and discussion

The 32 newly synthesized tertiary diarylamines (series **3–8**) were first evaluated for cytotoxic activity using a HTCL panel, including A549 (lung carcinoma), DU145 (prostate cancer), KB (epidermoid carcinoma of the nasopharynx), and KB_{VIN} (vincristine-resistant KB), with paclitaxel as a reference compound. The *in vitro* anticancer activity (GI₅₀) was determined using the established sulforhodamine B (SRB) method.¹² The cytotoxicity data of all new tertiary amines in HTCL assays are listed in Tables 1 and 2. Some of the designed tertiary diarylamine compounds were more potent than hit **1a** (GI₅₀ values 2.40–13.5) in the HTCL assays. As shown in Table 1, compounds **3a** with a *para*-methoxy ($R^1 = OMe$) and **3d** with a *para*-ester ($R^1 = COOMe$) on the phenyl ring displayed low micromolar GI₅₀ values ranging from 1.55 to 3.00 μM, and thus, were more potent than **3b** with a *para*-cyano (21–27 μM) and **3e** with 3,4-dimethoxy (15–18 μM) against the HTCL panel. However, corresponding compounds **3c** and **3f** with 4-trifluoromethoxy or 3,4,5-trimethoxy substitution, respectively, on the phenyl ring completely lost cytotoxic activity. These results indicated that a *para*-substituent on the phenyl ring could enhance the antiproliferative activity and a methoxy group was preferred to other substituents or multi-substituents on the phenyl ring. Consequently, in the series **4** compounds, the 4-methoxyphenyl moiety was retained, while the R^2 group on the linker was varied. In



Scheme 2. Synthesis of **8** series. (a) CH_3I , NaH (60% oil suspension), DMF, 0°C , 1 h; (b) (i) aq NaOH (3 N), THF/MeOH, rt, 36 h; (ii) HCl (2 N); (c) EtI or *i*-PrI, K_2CO_3 , acetone, reflux, 4 h; (d) NH_2Me , MeOH, rt, 4 days; (e) LiBH_4 , THF, MeOH, rt, 2 h; (f) CH_3I , NaH (60% oil suspension), THF, rt, 2 h; (g) NaN_3 , $\text{Et}_3\text{N}\cdot\text{HCl}$, toluene, reflux, 36 h; (h) Me_2SO_4 , K_2CO_3 , acetone, reflux, 5 h.

Table 1
Inhibitory activity of **3–4** against HTCL panel



	R^1	R^2	$\text{GI}_{50} \pm \text{SD}^a$ (μM)			
			A549	KB	KB_{VIN}	DU145
3a	4-OMe	Me	2.20 ± 0.20	1.78 ± 0.11	1.86 ± 0.30	1.55 ± 0.24
3b	4-CN	Me	24.0 ± 2.79	22.1 ± 2.52	27.0 ± 4.22	21.4 ± 3.89
3c	4-OCF ₃	Me	NA ^b	NA	NA	NA
3d	4-COOMe	Me	3.00 ± 0.35	2.89 ± 0.24	2.87 ± 0.55	2.22 ± 0.22
3e	3,4-diOMe	Me	18.4 ± 1.31	16.0 ± 0.62	16.5 ± 0.88	15.0 ± 0.95
3f	3,4,5-triOMe	Me	NA	NA	NA	NA
4a	4-OMe	Allyl	3.33 ± 0.41	2.61 ± 0.16	3.15 ± 0.57	2.69 ± 0.35
4b	4-OMe	<i>c</i> -Pentyl	NA	NA	NA	NA
4c	4-OMe	Ac	11.8 ± 2.36	14.3 ± 2.05	13.9 ± 1.25	11.2 ± 2.03
1a ^c	4-OMe	H	13.5	7.19	2.40	3.83
Paclitaxel ^c			8.18 ± 1.01 nM	7.77 ± 0.84 nM	1803 ± 302 nM	6.50 ± 0.43 nM

^a Concentration of compound that inhibits 50% human tumor cell growth, presented as mean \pm standard deviation (SD), performed at least in triplicate.

^b Not active; test compound (20 $\mu\text{g/mL}$) did not reach 50% inhibition.

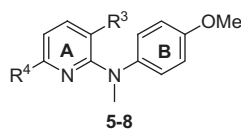
^c Positive control.

comparison with **3a** ($R^2 = \text{Me}$, GI_{50} 1.55–2.20 μM), compound **4a** with a *N*-allyl group showed comparable potency, but a bulky *N*-cyclopentyl group or an electron-withdrawing *N*-acetyl group resulted in significantly reduced or no potency (see **4b** and **4c**). Thus, as we expected, a small alkyl group on the linker might favor enhanced cytotoxic activity.

Next, we turned to modifications of the R^3 and R^4 substituents on the pyridine ring (A ring) (see Table 2). The R^4 on the pyridine ring was changed to methyl, methoxy, or *N*-methylamine, rather than the chlorine atom in **3a**. This change resulted in active compounds **5a–5c** with GI_{50} values of 2.70–9.63 μM . Then, because a nitro group is generally considered to be a moiety associated with risk and, thus, unacceptable in pharmaceutical agents,¹³ compounds **6a–6c** with a methoxy carbonyl (R^3) rather than the nitro group in the series **5** compounds and various R^4 groups (Cl, OMe, and NHMe, respectively) on the A-ring were synthesized and evaluated against the HTCL panel. Compound **6a** exhibited sub-micromolar GI_{50} values

(0.20–0.26 μM) and was ten-fold more potent than **3a** and **5a–c** (GI_{50} 1.55–9.63 μM), **6b** displayed similar potency to **5b**, while **6c** showed ten-fold higher potency against KB_{VIN} cell growth (GI_{50} 0.92 μM) compared with **5c** (GI_{50} 9.63 μM). The results from series **6** indicated that the R^3 on the pyridine ring can be modified to enhance potency and might have a greater impact on the potency than R^4 . Furthermore, two additional compound series, **7** (**a–g**) and **8** (**c–l**) with a chloro or trifluoromethyl R^4 group, respectively, were synthesized in parallel to investigate the impact of various R^3 groups on the antiproliferative activity. Among them, 3-methyl or -ethyl ester pyridine compounds **7b**, **8c**, and **8e** ($R^3 = \text{COOMe}$ or COOEt) showed high potency with low to sub-micromolar GI_{50} values (0.19–1.81 μM) similar to series **6**, regardless of whether R^4 was chloro or trifluoromethyl. In contrast, the presence of a 3-cyano (**7a** and **8j**), 3-isopropyl ester (**7d** and **8f**), 3-carboxylic acid (**7c** and **8d**), or 3-methylamide (**8g** and **7e**) on the pyridine ring resulted in substantially reduced ($\text{GI}_{50} > 7.21$ μM) or no cytotoxic activity. Therefore,

Table 2
Inhibitory activity of **5–8** against HTCL panel



	R ³	R ⁴	GI ₅₀ ± SD ^a (μM)			
			A549	KB	KB _{VIN}	DU145
3a	NO ₂	Cl	2.20 ± 0.20	1.78 ± 0.11	1.86 ± 0.30	1.55 ± 0.24
5a	NO ₂	Me	4.42 ± 0.44	2.92 ± 0.25	4.19 ± 0.97	3.35 ± 0.55
5b	NO ₂	OMe	3.27 ± 0.69	3.31 ± 0.46	2.83 ± 0.71	2.70 ± 0.25
5c	NO ₂	NHMe	4.50 ± 0.35	4.53 ± 0.70	9.63 ± 1.14	4.45 ± 0.85
6a	COOMe	Cl	0.23 ± 0.01	0.26 ± 0.04	0.20 ± 0.03	0.21 ± 0.04
6b	COOMe	OMe	3.15 ± 0.75	4.01 ± 0.75	4.02 ± 0.57	2.45 ± 0.49
6c	COOMe	NHMe	3.43 ± 0.30	1.36 ± 0.34	0.92 ± 0.09	1.67 ± 0.13
7a	CN	Cl	20.4 ± 2.51	22.1 ± 1.94	18.1 ± 3.73	20.4 ± 4.59
7b	COOEt	Cl	1.81 ± 0.12	1.80 ± 0.10	1.43 ± 0.18	1.43 ± 0.09
7c	COOH	Cl	NA ^b	NA	NA	NA
7d	COOPr- <i>i</i>	Cl	22.0 ± 1.64	14.5 ± 0.40	17.3 ± 1.58	17.8 ± 0.34
7e	CONHMe	Cl	NA	NA	NA	NA
7f	CH ₂ OH	Cl	3.25 ± 0.27	2.26 ± 0.10	2.12 ± 0.16	1.96 ± 0.11
7g	CH ₂ OMe	Cl	0.30 ± 0.03	0.33 ± 0.07	0.20 ± 0.01	0.25 ± 0.01
8c	COOMe	CF ₃	0.35 ± 0.05	0.41 ± 0.09	0.19 ± 0.01	0.25 ± 0.04
8d	COOH	CF ₃	NA	NA	NA	NA
8e	COOEt	CF ₃	1.46 ± 0.13	1.52 ± 0.10	1.30 ± 0.15	1.30 ± 0.13
8f	COOPr- <i>i</i>	CF ₃	NA	NA	NA	NA
8g	CONHMe	CF ₃	NA	NA	NA	NA
8h	CH ₂ OH	CF ₃	2.13 ± 0.09	1.92 ± 0.28	1.75 ± 0.11	1.71 ± 0.08
8i	CH ₂ OMe	CF ₃	1.20 ± 0.02	1.64 ± 0.04	1.43 ± 0.20	1.29 ± 0.11
8j	CN	CF ₃	7.21 ± 1.20	15.3 ± 2.33	7.91 ± 1.56	10.7 ± 2.49
8k		CF ₃	NA	NA	NA	NA
8l		CF ₃	1.82 ± 0.50	1.47 ± 0.34	1.26 ± 0.09	1.16 ± 0.05
Paclitaxel ^c			8.18 ± 1.01 nM	7.77 ± 0.84 nM	1803 ± 302 nM	6.50 ± 0.43 nM

^a Concentration of compound that inhibits 50% human tumor cell growth, presented as mean ± standard deviation (SD), performed at least in triplicate.

^b Not active; test compound (20 μg/mL) did not reach 50% inhibition.

^c Positive control.

while a methyl or ethyl ester R³ group was beneficial, a bulky (isopropyl ester) or negatively charged (such as carboxylic acid at physiological pH) R³ substituent impaired the cytotoxic activity. Interestingly, we observed that 3-methoxymethylpyridines **7g** and **8i** (R³ = CH₂OMe) and 3-hydroxymethylpyridines **7f** and **8h** (R³ = CH₂OH) also were potent with GI₅₀ values of 0.20–3.25 μM, generally comparable with 3-methyl and -ethyl ester compounds. Notably, compounds **6a** (R³ = COOMe, R⁴ = Cl), **7g** (R³ = CH₂OMe, R⁴ = Cl), and **8c** (R³ = COOMe, R⁴ = CF₃) exhibited GI₅₀ values between 0.19 and 0.41 μM against all four HTCL. Similarly to **7c** and **8d**, compound **8k** with a 3-tetrazole ring, a bio-isostere of a carboxylic acid, on the pyridine ring was inactive. However, with a methylated tetrazole that cannot ionize, compound **8l** exhibited high potency with low micromolar GI₅₀ values ranging from 1.16 to 1.82 μM against the HTCL panel.

More interestingly, we found that most active compounds in the series of tertiary diarylamine showed equal or slightly better potency against both the KB and paclitaxel-resistant KB_{VIN} cell lines (see **Tables 1 and 2**). In contrast, paclitaxel showed nanomolar activity against KB cells (GI₅₀ 8 nM), but significantly lower potency (GI₅₀ 1800 nM) against the KB_{VIN} cell line, which over-expresses P-glycoprotein, a drug efflux transporter. These results indicated that these types of active compounds are not substrates

of P-glycoprotein and can overcome paclitaxel-resistance, providing a therapeutic advantage over paclitaxel.

In investigating possible biological target(s), the three most active compounds **6a**, **7g**, and **8c** (GI₅₀ 0.19–0.41 μM) were tested in tubulin assays. As shown in **Table 3**, they showed high activity for inhibition of tubulin assembly, with IC₅₀ values ranging from 1.4 to 1.7 μM, which are comparable to those with CA-4 (IC₅₀ 1.2 μM), a tubulin inhibitor currently in phase II clinical trials, in the same assay. Furthermore, they inhibited the binding of colchicine to tubulin (≥80%). These results suggest that these active diarylamines might exert their effects by inhibiting tubulin polymerization targeted at the colchicine binding site.

To better understand how the diarylamine analogues interact with tubulin, we investigated the binding mode of **6a** at the colchicine binding domain in the tubulin dimer by using CDOCKER in the Discovery Studio 3.0 software. We attempted to dock **6a** into two different crystal structures, the tubulin/TN16 complex (PDB ID code: 3HKD) and the tubulin/DMDA-colchicine complex (PDB ID code: 1SA0). We selected the former crystal structure as our modeling system, because **6a** showed a lower binding energy (−14.50 kcal/mol) in 3HKD than in 1SA0 (−9.74 kcal/mol) and superposed very well with the native ligand TN16 in the 3HKD

Table 3
Inhibition of tubulin assembly^a and colchicine binding^b

compound	inhibition of tubulin assembly IC ₅₀ (μM) ± SD	inhibition of colchicine binding (%) ± SD
6a	1.40 ± 0.01	80 ± 2.0
7g	1.50 ± 0.20	88 ± 0.5
8c	1.70 ± 0.20	82 ± 1.0
CA-4 ^c	1.20 ± 0.20	98 ± 0.6

^a The tubulin assembly assay measured the extent of assembly of 10 μM tubulin after 20 min at 30 °C.

^b Tubulin: 1 μM. [³H]colchicine: 5 μM. Inhibitor: 5 μM. Incubation was performed for 10 min at 37 °C.

^c Reference compound is a drug candidate in phase II clinical trial.

structure. Figure 3A illustrates the binding mode of **6a** (orange) with tubulin protein and its overlap with TN16 (cyan). The methoxy group on the B-ring of **6a** formed two hydrogen bonds with the carboxyl group of Glu200 and the hydroxyl of Tyr202 in β-S6, while TN-16 formed one H-bond also with Glu200 and another H-bond with Val238 in β-H7. The pyridine moiety (A-ring) of **6a** bound in the lipophilic pocket formed by the side chains of amino acids in β-S8 and β-H7, and the ester group on the A-ring showed two hydrogen bonds with the side chain of Cys241, a key amino acid in the colchicine binding site. For comparison, we superposed **6a**, DMDA-colchicine (the native ligand of 1SA0), and CA-4 into the same docking model, as shown in Figure 3B. While the TN16 binding site extended deeply into the β-subunit side and less into the α-subunit,^{14,15} DMDA-colchicine (green) and CA-4 (blue) bound at the interface between the α- and β-subunits of the tubulin dimer, and showed an overlap only with the pyridine ring of **6a**. The 3,4,5-trimethoxyphenyl moieties found in both DMDA-colchicine and CA-4 overlapped well and also formed H-bonds with the thiol group of Cys241, which plays a locating role for most tubulin inhibitors binding at the colchicine binding site. The theoretical model of **6a** supports our bioassay results and can explain, at least partially, the high potency of **6a** and the preference for the ester group on the pyridine ring. Meanwhile, it also reveals obvious differences in the binding conformations and orientations between our active compounds and CA-4 in the colchicine binding site.

In summary, three new leads **6a**, **7g**, and **8c** exhibited promising cytotoxic activity in human tumor cell line assays with submi-

cromolar GI₅₀ values, significant potency against tubulin assembly, and inhibitory activity for colchicine binding to tubulin protein. Notably, the active tertiary diarylamine compounds showed high potency against paclitaxel-resistant KB_{VIN} cell lines, providing a potential advantage over paclitaxel. In addition, molecular modeling studies revealed that the active **6a** and CA-4 might have different binding modes. Therefore, our active tertiary diarylamines might be a novel class of tubulin inhibitors targeting the colchicine binding site. Current SAR studies on several series of *N*-methyl-*N*-(4-methoxyphenyl)pyridin-2-amines revealed the following conclusions: (1) a tertiary amine linker is crucial for enhanced antitumor activity, and a methyl group is better than others, (2) a *para*-methoxyphenyl moiety is favorable for antitumor activity, (3) the R³ group on the pyridine ring can be modified to improve potency, and methyl ester and methoxymethyl groups are better than other groups tested, (4) the R⁴ substituent on the pyridine ring also contributes to the cytotoxic activity, but seems to have less impact than R³. We will use these initial promising results to guide our further optimization of new compounds as tubulin inhibitors targeting the colchicine binding site. In addition, because various tubulin inhibitors targeting the colchicine binding site have been reported to selectively disrupt the cytoskeleton of proliferating endothelial cells as vascular disrupting agents (VDAs),^{16,17} further studies on our newly discovered active compounds will be necessary to develop a new class of antitumor drug with a new mechanism of action as a new approach for treating cancers and tumors.

4. Experimental section

4.1. Chemistry

The nuclear magnetic resonance (¹H and ¹³C NMR) spectra were measured on a JNM-ECA-400 (400 MHz and 100 MHz, respectively) spectrometer using tetramethylsilane (TMS) as internal standard. The solvent used was CDCl₃ unless otherwise indicated. Mass spectra (MS) were measured on API-150 mass spectrometer with the electrospray ionization source from ABI, Inc. Melting points were measured with a RY-1 melting apparatus without correction. The microwave reactions were performed on a microwave reactor from Biotage, Inc. Medium-pressure column chromatogra-

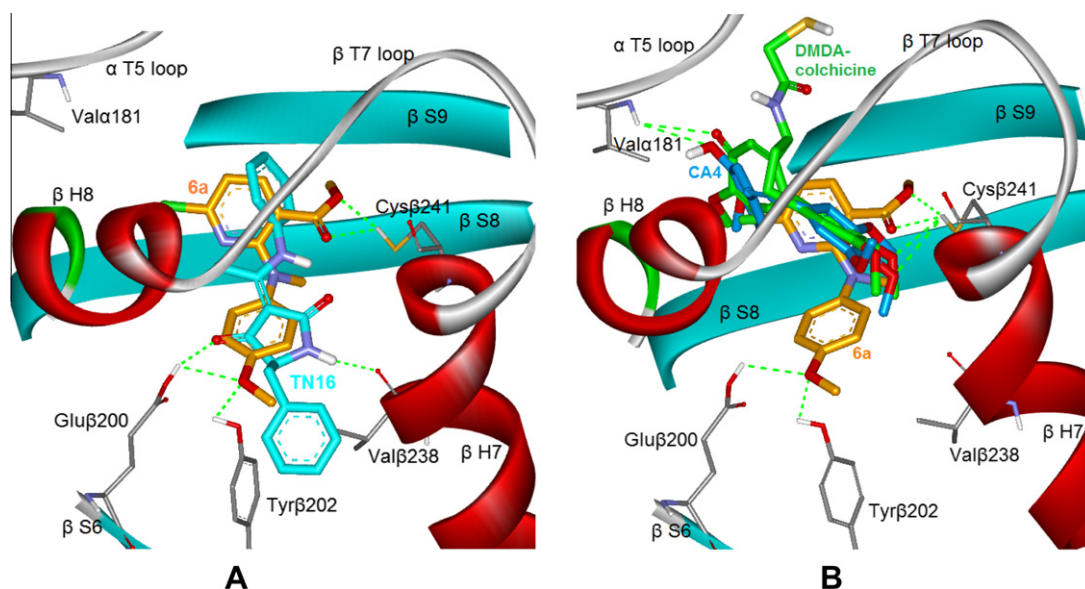


Figure 3. (A) A predicted mode of compound **6a** (orange stick model) binding with tubulin (PDB ID code: 3HKD), and overlapping with TN16 (cyan stick model, the native ligand of 3HKD); (B) the superimposition of docked compound **6a** with DMDA-colchicine (green stick model, the native ligand of 1SA0) and CA-4 (blue stick model). Surrounding amino acid side chains are shown in gray stick format and labeled. The hydrogen bonds are shown by green dashed lines and the distance between the ligands and protein is less than 3 Å

phy was performed using a CombiFlash® Companion system from ISCO, Inc. Thin-layer chromatography (TLC) was performed on silica gel GF254 plates. Silica gel GF254 and H (200–300 mesh) from Qingdao Haiyang Chemical Company were used for TLC, preparative TLC (PTLC), and column chromatography, respectively. All commercial chemical reagents were purchased from Beijing Chemical Works or Sigma–Aldrich, Inc. Purities of target compounds were determined by using an Agilent HPLC-1200 with UV detector and an Agilent Eclipse XDB-C18 column (150 mm × 4.6 mm, 5 µm) eluting with a mixture of solvents A and B (acetonitrile/water 80:20), flow rate 0.8 mL/min and UV detection at 254 nm.

4.2. 6-Chloro-*N*-(4-cyanophenyl)-*N*-methyl-3-nitropyridin-2-amine (3b)

A mixture of 2,6-dichloro-3-nitropyridine (**2a**, 94 mg, 0.5 mmol) and *N*-methyl 4-cyanoaniline (80 mg, 0.6 mmol) was heated neat at 120 °C under N₂ protection for 4 h with stirring. Then the mixture was diluted with CH₂Cl₂ and purified by preparative TLC (CH₂Cl₂/petroleum ether/MeOH = 1/1.5/0.04) to obtain 40 mg of **3b** in 37% yield, together with recovery of 24 mg of **2a**, yellow solid, mp 98–100 °C; ¹H NMR δ ppm 3.66 (3H, s, NCH₃), 7.02 (1H, d, *J* = 8.4 Hz, PyH-5), 7.09 (2H, d, *J* = 8.8 Hz, ArH-2',6'), 7.58 (2H, d, *J* = 8.8 Hz, ArH-3',5'), 8.07 (1H, d, *J* = 8.4 Hz, PyH-4); MS *m/z* (%) 289 (M+1, 100), 291 (M+3, 35); HPLC purity 97.7%.

4.3. General procedure for coupling of substituted 2-chloropyridine and *N*-alkylaniline

Method A (traditional): A mixture of a substituted 2-chloropyridine (**2**, 1.0 mmol), *N*-methyl-4-methoxyaniline (1.5 mmol), and anhydrous potassium carbonate (2 mmol) in *t*-BuOH was stirred at rt for 12–24 h monitored by TLC until the reaction was complete. The mixture was poured into ice-water, the pH adjusted to ca. 3.0 with aq HCl (2 N), and the resulting solution extracted with CH₂Cl₂ three times. The combined organic phases were washed with water and brine, successively, until neutral and dried over anhydrous Na₂SO₄ overnight. After removal of solvent in vacuo, the crude product was purified by flash column chromatography (gradient elution: EtOAc/petroleum ether, 0–50%) to obtain corresponding pure product. **Method B (microwave irradiation):** A mixture of **2** (1.0 mmol), substituted aniline (1.5 mmol), and anhydrous potassium carbonate (414 mg, 3.0 mmol) in 3 mL of *t*-BuOH was heated at 120–160 °C with microwave-assistance for 10–30 min with stirring. The reaction mixture was then poured into ice-water, pH adjusted to ~3.0 with aq HCl (2 N), and solid crude product was filtered. The product was then purified by the same methods as in Method A above.

4.4. 6-Chloro-*N*-(4-methoxyphenyl)-*N*-methyl-3-nitropyridine-2-amine (3a)

Method A. Starting with 193 mg of **2a** and 206 mg of *N*-methyl 4-methoxyaniline to produce 240 mg of **3a**, 82% yield, orange solid recrystallized from MeOH, mp 96–97 °C; ¹H NMR δ ppm 3.54 (3H, s, NCH₃), 3.78 (3H, s, OCH₃), 6.76 (1H, d, *J* = 8.4 Hz, PyH-5), 6.83 (2H, d, *J* = 9.2 Hz, ArH-2',6'), 7.00 (2H, d, *J* = 9.2 Hz, ArH-3',5'), 7.88 (1H, d, *J* = 8.4 Hz, PyH-4); MS *m/z* (%) 294 (M+1, 100), 296 (M+3, 32); HPLC purity 99.5%.

4.5. 6-Chloro-*N*-methyl-3-nitro-*N*-(4-trifluoromethoxyphenyl)pyridin-2-amine (3c)

Method B. Starting with 193 mg of **2a** and 288 mg of *N*-methyl-4-trifluoromethoxyaniline at 120 °C for 30 min to produce 198 mg of **3c**, 57% yield, yellow liquid. ¹H NMR δ ppm 3.59 (1H, s, NCH₃), 6.87 (1H, d, *J* = 8.4 Hz, PyH-5), 7.08 (2H, d, *J* = 8.8 Hz, ArH-2',6'),

7.16 (2H, d, *J* = 8.8 Hz, ArH-3',5'), 7.96 (1H, d, *J* = 8.4 Hz, PyH-4); MS *m/z* (%) 348 (M+1, 100), 350 (M+3, 25); HPLC purity 97.2%.

4.6. 6-Chloro-*N*-methyl-*N*-(4-methoxycarbonylphenyl)-3-nitropyridin-2-amine (3d)

Method B. Starting with 193 mg of **2a** and 248 mg of methyl *N*-methyl-4-amino benzoate at 160 °C for 15 min to produce 130 mg of **3d**, 41% yield, brown solid, mp 106–107 °C; ¹H NMR δ ppm 3.67 (1H, s, NCH₃), 3.89 (1H, s, OCH₃), 6.94 (1H, d, *J* = 8.4 Hz, PyH-5), 7.07 (2H, d, *J* = 9.2 Hz, ArH-2',6'), 7.98 (2H, d, *J* = 9.2 Hz, ArH-3',5'), 8.02 (1H, d, *J* = 8.4 Hz, PyH-4); MS *m/z* (%) 322 (M+1, 100), 324 (M+3, 28); HPLC purity 97.2%.

4.7. 6-Chloro-*N*-(3,4-dimethoxyphenyl)-*N*-methyl-3-nitropyridin-2-amine (3e)

Method A. Starting with 193 mg of **2a** and 250 mg of *N*-methyl-3,4-dimethoxyaniline to produce 262 mg of **3e**, 81% yield, red solid, mp 145–146 °C; ¹H NMR δ ppm 3.56 (s, 3H, NCH₃), 3.83 (s, 3H, OCH₃), 3.85 (s, 3H, OCH₃), 6.60 (2H, m, ArH-2' and 6'), 6.78 (1H, d, *J* = 8.0 Hz, PyH-5), 6.80 (1H, d, *J* = 9.2 Hz, ArH-4'), 7.88 (1H, d, *J* = 8.0 Hz, PyH-4); MS *m/z* (%) 324.3 (M+1, 18), 325.9 (M+3, 6), 290.1 (M–33, 100); HPLC purity 99.2%.

4.8. 6-Chloro-*N*-methyl-3-nitro-*N*-(3,4,5-trimethoxyphenyl)pyridin-2-amine (3f)

Method A. Starting with 193 mg of **2a** and 250 mg of *N*-methyl-3,4,5-trimethoxyaniline to produce 268 mg of **3f**, 76% yield, orange solid, mp 138–140 °C; ¹H NMR δ ppm 3.60 (3H, s, NCH₃), 3.79 (3H, s, OCH₃), 3.80 (3H, s, OCH₃), 3.83 (3H, s, OCH₃), 6.26 (2H, s, ArH-2',6'), 6.82 (1H, d, *J* = 8.4 Hz, PyH-5), 7.91 (1H, d, *J* = 8.4 Hz, PyH-4); MS *m/z* (%) 324.3 (M+1, 18), 325.9 (M+3, 6), 290.1 (M–33, 100); HPLC purity 99.5%.

4.9. *N*-Allyl-6-chloro-*N*-(4-methoxyphenyl)-3-nitropyridin-2-amine (4a)

Method B. Starting with 193 mg of **2a** and 244 mg of *N*-allyl-4-methoxyaniline at 120 °C for 10 min to produce 168 mg of **4a**, 53% yield, red liquid. ¹H NMR δ ppm 3.77 (3H, s, OCH₃), 4.63 (2H, d, *J* = 5.6 Hz, NCH₂), 5.16 and 5.18 (each 1H, dd, *J* = 17.6 Hz and 1.2 Hz, CH₂=), 5.99 (1H, m, CH), 6.76 (1H, d, *J* = 8.4 Hz, PyH-5), 6.81 (2H, d, *J* = 9.2 Hz, ArH-2',6'), 6.98 (2H, d, *J* = 9.2 Hz, ArH-3',5'), 7.87 (1H, d, *J* = 8.4 Hz, PyH-4); MS *m/z* (%) 320 (M+1, 100), 322 (M+3, 25); HPLC purity 99.4%.

4.10. 6-Chloro-*N*-cyclopentyl-*N*-(4-methoxyphenyl)-3-nitropyridin-2-amine (4b)

Method B. Starting with 194 mg of **2a** and 288 mg of *N*-cyclopentyl-*N*-4-methoxyaniline at 160 °C for 20 min to produce 196 mg of **4b**, 50% yield, yellow solid, mp 93–94 °C; ¹H NMR δ ppm 1.49–1.61 (6H, m, CH₂ × 3), 2.02 (2H, m, CH₂), 3.79 (1H, s, OCH₃), 4.93 (1H, m, CH), 6.70 (1H, d, *J* = 8.0 Hz, PyH-5), 6.83 (2H, d, *J* = 9.2 Hz, ArH-2',6'), 6.93 (2H, d, *J* = 9.2 Hz, ArH-3',5'), 7.69 (1H, d, *J* = 8.0 Hz, PyH-4); MS *m/z* (%) 348 (M+1, 100), 350 (M+3, 32); HPLC purity 98.7%.

4.11. *N*-(4-Methoxyphenyl)-*N*-methyl-6-methyl-3-nitropyridin-2-amine (5a)

Method B. Starting with 174 mg of **2b** and 206 mg of *N*-methyl-4-methoxyaniline at 140 °C for 20 min to produce 154 mg of **5a**, 56% yield, yellow solid, mp 97–98 °C; ¹H NMR δ ppm 2.53 (3H, s,

CH₃), 3.53 (3H, s, NCH₃), 3.77 (3H, s, OCH₃), 6.64 (1H, d, *J* = 8.0 Hz, PyH-5), 6.82 (2H, d, *J* = 9.2 Hz, ArH-2',6'), 6.99 (2H, d, *J* = 9.2 Hz, ArH-3',5'), 7.86 (1H, d, *J* = 8.0 Hz, PyH-4); MS *m/z* (%) 274 (M+1, 100); HPLC purity 98.5%.

4.12. Methyl 6-chloro-2-(*N*-(4-methoxyphenyl)-*N*-methyl)aminonicotinate (6a)

Method B. Starting with 206 mg of methyl 2,6-dichloronicotinate (**2c**) and 206 mg of *N*-methyl-4-methoxyaniline at 160 °C for 30 min to produce 186 mg of **6a**, 60% yield, pale yellow solid, mp 79–81 °C; ¹H NMR δ ppm 3.28 (3H, s, NCH₃), 3.47 (3H, s, OCH₃), 3.78 (3H, s, OCH₃), 6.74 (1H, d, *J* = 8.0 Hz, PyH-5), 6.84 (2H, d, *J* = 9.2 Hz, ArH-2',6'), 7.02 (2H, d, *J* = 9.2 Hz, ArH-3',5'), 7.61 (1H, d, *J* = 8.0 Hz, PyH-4); ¹³C NMR δ ppm 41.23, 51.79, 55.57, 113.21, 114.07, 114.74, 115.45, 125.55, 128.34, 141.30, 141.72, 151.33, 156.81, 156.98, 167.35; MS *m/z* (%) 307 (M+1, 100), 309 (M+3, 29); HPLC purity 99.2%.

4.13. 6-Chloro-3-cyano-*N*-(4-methoxyphenyl)-*N*-methylpyridin-2-amine (7a)

Method B. Starting with 173 mg of 3-cyano-2,6-dichloropyridine (**2e**) and 205 mg of *N*-methyl-4-methoxyaniline at 160 °C for 15 min to produce 32 mg of **7a**, 12% yield, white solid, mp 137–138 °C; ¹H NMR δ ppm 3.47 (3H, s, NCH₃), 3.85 (3H, s, OCH₃), 6.18 (1H, d, *J* = 8.4 Hz, PyH-5), 6.99 (2H, d, *J* = 8.8 Hz, ArH-2',6'), 7.14 (2H, d, *J* = 8.8 Hz, ArH-3',5'), 7.38 (1H, d, *J* = 8.4 Hz, PyH-4). MS *m/z* (%): 274 (M+1, 100), 276 (M+3, 31); HPLC purity 99.0%.

4.14. Ethyl 6-chloro-2-(*N*-(4-methoxyphenyl)-*N*-methyl)aminonicotinate (7b)

Method B. Starting with 220 mg of ethyl 2,6-dichloronicotinate (**2d**) and 205 mg of *N*-methyl-4-methoxyaniline at 160 °C for 30 min to produce 173 mg of **7b**, 54% yield, yellow solid, mp 79–81 °C; ¹H NMR δ ppm 1.08 (3H, t, *J* = 7.6 Hz, CH₃), 3.47 (3H, s, NCH₃), 3.70 (2H, q, *J* = 7.2 Hz, CH₂), 3.78 (3H, s, OCH₃), 6.73 (2H, d, *J* = 8.0 Hz, PyH-5), 6.83 (2H, d, *J* = 9.2 Hz, ArH-2',6'), 7.03 (2H, d, *J* = 9.2 Hz, ArH-3',5'), 7.61 (1H, d, *J* = 8.0 Hz, PyH-4); MS *m/z* (%) 321.3 (M+1, 58), 323.3 (M+3, 20), 275.1 (M–45, 100); HPLC purity 96.7%.

4.15. 6-Chloro-*N*-(4-methoxyphenyl)-*N*-methylcarbonyl-3-nitropyridin-2-amine (4c)

To a solution of **2a** (280 mg, 1.0 mmol) in Ac₂O (8 mL) was added a drop of concentrated H₂SO₄. The mixture was heated at 100 °C under N₂ protection for 18 h with stirring. After the reaction was completed, the mixture was poured into ice-water and neutralized with 5% aq NaOH. The collected solid was further purified by flash chromatography (gradient eluant/EtOAc/petroleum ether, 0–50%) to obtain 249 mg of pure **4c**, 77% yield, yellow solid, mp 146–147 °C; ¹H NMR δ ppm 2.01 (3H, s, CH₃), 3.86 (3H, s, OCH₃), 6.99 (2H, d, *J* = 8.8 Hz, ArH-2',6'), 7.31 (1H, d, *J* = 8.4 Hz, PyH-5), 7.49 (2H, d, *J* = 8.8 Hz, ArH-3',5'), 8.22 (1H, d, *J* = 8.4 Hz, PyH-4); MS *m/z* (%) 322 (M+1, 100), 324 (M+3, 28); HPLC purity 97.8%.

4.16. 6-Methoxy-*N*-(4-methoxyphenyl)-*N*-methyl-3-nitropyridin-2-amine (5b)

A mixture of **3a** (117 mg, 0.4 mmol) and NaOMe (ca. 1.0 mmol) in 3 mL of MeOH was refluxed for 2 h with stirring. After the reaction was finished, the mixture was poured into ice-water to obtain 108 mg of pure **5b** as a yellow solid, 93% yield, mp 56–57 °C; ¹H NMR δ ppm 3.54 (3H, s, NCH₃), 3.78 (3H, s, OCH₃), 3.99 (3H, s,

OCH₃), 6.19 (1H, d, *J* = 8.8 Hz, PyH-5), 6.83 (2H, d, *J* = 9.2 Hz, ArH-2',6'), 7.02 (2H, d, *J* = 9.2 Hz, ArH-3',5'), 8.03 (1H, d, *J* = 8.8 Hz, PyH-4); MS *m/z* (%) 290 (M+1, 100); HPLC purity 95.6%.

4.17. Methyl 6-methoxy-2-(*N*-(4-methoxyphenyl)-*N*-methyl)aminonicotinate (6b)

Prepared in the same manner as for **5b**. Starting with 123 mg of **6a** to obtain 119 mg of **6b** in 98% yield, white solid, mp 78–80 °C; ¹H NMR δ ppm 3.28 (3H, s, NCH₃), 3.48 (3H, s, OCH₃), 3.78 (3H, s, OCH₃), 3.96 (3H, s, OCH₃), 6.18 (1H, d, *J* = 8.4 Hz, PyH-5), 6.83 (2H, d, *J* = 9.2 Hz, ArH-2',6'), 7.03 (2H, d, *J* = 9.2 Hz, ArH-3',5'), 7.71 (1H, d, *J* = 8.4 Hz, PyH-4). MS *m/z* (%) 303 (M+1, 24), 271 (M–31, 100); HPLC purity 97.9%.

4.18. *N*²,*N*⁶-Dimethyl-*N*-(4-methoxyphenyl)-3-nitropyridin-2,6-diamine (5c)

Compound **3a** (117 mg, 0.2 mmol) in 3 mL of 30% methylamine-MeOH solution was refluxed for 12 h with stirring. After the reaction was completed, the mixture was poured into ice-water, and the resulting red solid was collected to give 86 mg of pure **5c**, 75% yield, mp 169–170 °C; ¹H NMR δ ppm 3.03 (3H, d, *J* = 5.2 Hz, NCH₃), 3.49 (3H, s, NCH₃), 3.76 (3H, s, OCH₃), 5.01 (1H, br s, NH), 5.87 (1H, d, *J* = 9.2 Hz, PyH-5), 6.81 (2H, d, *J* = 8.8 Hz, ArH-2',6'), 7.02 (2H, d, *J* = 8.8 Hz, ArH-3',5'), 8.00 (1H, d, *J* = 9.2 Hz, PyH-4); MS *m/z* (%) 289 (M+1, 27), 255 (M–33, 100); HPLC purity 100.0%.

4.19. Methyl 2-[*N*-(4-methoxyphenyl)-*N*-methyl]amino-6-methylaminonicotinate (6c)

Prepared in the same manner as for **5c**. Starting with 123 mg of **6a** to obtain 96 mg of **6c**, 80% yield, white solid, mp 88–90 °C; ¹H NMR δ ppm 2.97 (3H, d, *J* = 5.2 Hz, NHCH₃), 3.28 (3H, s, NCH₃), 3.43 (3H, s, OCH₃), 3.76 (3H, s, OCH₃), 4.69 (1H, br s, NH), 5.88 (1H, d, *J* = 8.8 Hz, PyH-5), 6.80 (2H, d, *J* = 9.2 Hz, ArH-2',6'), 7.01 (2H, d, *J* = 9.2 Hz, ArH-3',5'), 7.67 (1H, d, *J* = 8.8 Hz, PyH-4); MS *m/z* (%) 302 (M+1, 1), 227 (M–7, 100); HPLC purity 100.0%.

4.20. 6-Chloro-2-(*N*-(4-methoxyphenyl)-*N*-methyl)aminonicotinic acid (7c)

To a solution of **6a** (154 mg, 0.5 mmol) in THF/MeOH (1.5 mL/1.5 mL) was added 3 N aq NaOH (3.0 mL) dropwise with stirring at rt for 36 h. The mixture was poured into 20 mL of water. After removal of insoluble substance, the water phase was acidified with aq. HCl (2 N) to pH 2. The precipitated solid was collected, washed with water, and dried to give 112 mg of pure **7c**, 77% yield, yellow solid, mp 138–140 °C; ¹H NMR δ ppm 3.43 (3H, s, OCH₃), 3.72 (3H, s, OCH₃), 6.81 (2H, d, *J* = 8.8 Hz, ArH-2',6'), 6.90 (1H, d, *J* = 8.0 Hz, PyH-5), 7.00 (2H, d, *J* = 8.8 Hz, ArH-3',5'), 7.90 (1H, d, *J* = 8.0 Hz, PyH-4). MS *m/z* (%) 293.2 (M+1, 100), 295.3 (M+3, 45); HPLC purity 95.2%.

4.21. Isopropyl 6-chloro-2-(*N*-(4-methoxyphenyl)-*N*-methyl)aminonicotinate (7d)

A mixture of **7c** (59 mg, 0.2 mmol), *i*-PrI (68 mg, 0.4 mmol), and K₂CO₃ (55 mg, 0.4 mmol) in 5 mL of acetone was refluxed for 4 h. K₂CO₃ was filtered out, and acetone was removed under reduced pressure. The solid residue was purified by flash column chromatography (gradient eluant/EtOAc/petroleum ether, 0–40%) to give 55 mg of pure **7d**, 82% yield, pale yellow solid, mp 56–58 °C; ¹H NMR δ ppm 1.02 (6H, d, *J* = 6.0 Hz, CH₃×2), 3.46 (3H, s, NCH₃), 3.76 (3H, s, OCH₃), 4.60 (1H, m, CH), 6.73 (1H, d, *J* = 8.0 Hz, PyH-5), 6.82 (2H, d, *J* = 9.2 Hz, ArH-2',6'), 7.02 (2H, d, *J* = 9.2 Hz, ArH-

3',5'), 7.59 (1H, d, J = 8.0 Hz, PyH-4); MS m/z (%) 335.4 (M+1, 32), 337.3 (M+3, 11), 275.1 (M–59⁺, 100); HPLC purity 95.5%.

4.22. *N*-Methyl 6-chloro-2-(*N*-(4-methoxyphenyl)-*N*-methyl)aminonicotinamide (7e)

A mixture of **7c** (84 mg, 0.29 mmol), EDCI (86 mg, 0.45 mmol) and HOBt (61 mg, 0.45 mmol) in CH₂Cl₂ (4 mL) was stirred at rt for 30 min, and then 30% methyl amine (0.18 mL)–MeOH solution was added dropwise at 0 °C with stirring over 15 min, followed by warming to rt for an additional 90 min. After adding water (20 mL), the product was extracted with CH₂Cl₂ three times. The combined organic phase was washed with water and brine, successively, and dried over anhydrous Na₂SO₄ overnight. After removal of solvent in vacuo, crude product was purified by flash column chromatography (gradient eluant/EtOAc/petroleum ether, 0–50%) to give 59 mg of pure **7e**, 66% yield, white solid, mp 150–152 °C; ¹H NMR δ ppm 2.52 (3H, d, J = 7.2 Hz, NHCH₃), 3.39 (3H, s, NCH₃), 3.77 (3H, s, OCH₃), 6.16 (1H, br, NH), 6.83 (2H, d, J = 8.8 Hz, ArH-2',6'), 6.90 (1H, d, J = 7.6 Hz, PyH-5), 6.95 (2H, d, J = 8.8 Hz, ArH-3',5'), 7.74 (1H, d, J = 7.6 Hz, PyH-4); MS m/z (%) 306 (M+1, 16), 308 (M+3, 6), 275.1 (M–30, 100); HPLC purity 98.3%.

4.23. 6-Chloro-3-hydroxymethyl-*N*-(4-methoxyphenyl)-*N*-methylpyridin-2-amine (7f)

To a solution of **6a** (123 mg, 0.4 mmol) in 5 mL of anhydrous THF, LiBH₄ (88 mg, 4.0 mmol) was added at 0 °C with stirring over 15 min, and then the solution was warmed to rt for 30 min. MeOH (0.5 mL) was then added dropwise to the mixture with stirring for an additional 30 min. The mixture was poured into ice-water and extracted with EtOAc three times. Combined organic phase was washed successively with water and brine, and dried over anhydrous Na₂SO₄ overnight. After removal of solvent in vacuo, the crude product was purified by flash column chromatography (gradient eluant/EtOAc/petroleum ether, 0–50%) to produce 91 mg of pure **7f**, 82% yield, yellow oil. ¹H NMR δ ppm 3.35 (3H, s, NCH₃), 3.79 (3H, s, OCH₃), 3.98 (2H, s, CH₂), 6.84 (2H, d, J = 8.8 Hz, ArH-2',6'), 6.92 (1H, d, J = 8.0 Hz, PyH-4), 6.95 (2H, d, J = 8.8 Hz, ArH-3',5'), 7.60 (1H, d, J = 8.0 Hz, PyH-5); MS m/z (%) 279.2 (M+1, 100), 281.2 (M+3, 34); HPLC purity 99.4%.

4.24. 6-Chloro-3-methoxymethyl-*N*-(4-methoxyphenyl)-*N*-methylpyridin-2-amine (7g)

To a solution of **7f** (51 mg, 0.18 mmol) and Mel (0.03 mL, 0.54 mmol) in 6 mL of anhydrous THF was added NaH (22 mg, 0.54 mmol, 60% oil suspension) at 0 °C and stirred for 30 min at 0 °C and for 2 h at rt. The mixture was poured into ice-water and extracted with EtOAc three times. The combined organic phase was washed with water and brine, successively, and dried over anhydrous Na₂SO₄ overnight. After removal of solvent in vacuo, the crude product was purified by flash column chromatography (gradient eluant/EtOAc/petroleum ether, 0–30%) to give 41 mg of pure **7g**, 78% yield, yellow oil. ¹H NMR δ ppm 3.15 (3H, s, OCH₃), 3.36 (3H, s, NCH₃), 3.69 (2H, s, OCH₂), 3.79 (3H, s, OCH₃), 6.82 (2H, d, J = 8.8 Hz, ArH-2',6'), 6.91 (3H, m, PyH-5 and ArH-3',5'), 7.58 (1H, d, J = 8.0 Hz, PyH-4); ¹³C NMR δ ppm 42.07, 55.45, 58.29, 70.16, 114.59, 115.12, 116.09, 122.63, 125.09, 128.22, 138.86, 142.20, 147.50, 156.27, 157.05; MS m/z (%) 261 (M–31⁺, 100), 293 (M+1, 52), 295.3 (M+3, 18); HPLC purity 99.3%.

4.25. Methyl 2-(*N*-(4-methoxyphenyl)-*N*-methyl)amino-6-trifluoromethylnicotinate (8c)

To a solution of methyl 6-chloro-2-[*N*-(4-methoxyphenyl) amino]-6-trifluoro-methylnicotinate (**8a**, 120 mg, 0.37 mmol), and

Mel (0.07 mL, 1.13 mmol) in DMF (3–5 mL) was added NaH (44 mg, 1.1 mmol, 60% oil suspension) at 0 °C with stirring for 1 h. After the reaction was completed, the mixture was poured into ice-water and extracted with EtOAc three times. The combined organic phase was washed with water and brine successively, and dried over anhydrous Na₂SO₄ overnight. After removal of solvent in vacuo, the crude product was purified by flash chromatography (gradient eluant/EtOAc/petroleum ether, 0–50%) to produce 116 mg of **8c**, 92% yield, yellow solid, mp 99–101 °C; ¹H NMR δ ppm 3.30 (3H, s, NCH₃), 3.50 (3H, s, OCH₃), 3.79 (3H, s, OCH₃), 6.85 (2H, d, J = 9.2 Hz, ArH-2',6'), 7.04 (2H, d, J = 9.2 Hz, ArH-3',5'), 7.06 (1H, d, J = 8.0 Hz, PyH-5), 7.74 (1H, d, J = 8.0 Hz, PyH-4); ¹³C NMR δ ppm 40.94, 51.83, 55.47, 109.46, 114.66 (2C), 118.36, 125.78 (2C), 140.10, 140.92, 147.63, 147.97, 156.32, 157.05, 167.19; MS m/z (%) 341 (M+1, 6), 309 (M–31, 100); HPLC purity 97.2%.

4.26. 2-(*N*-(4-Methoxyphenyl)-*N*-methyl)amino-6-trifluoromethylnicotinic acid (8d)

Prepared in a similar manner as for **7c**. Starting with 170 mg of **8c** to produce 118 mg of **8d**, 72% yield, mp 146–148 °C; ¹H NMR δ ppm 3.48 (3H, s, NCH₃), 3.71 (3H, s, OCH₃), 6.80 (2H, d, J = 8.8 Hz, ArH-2',6'), 7.02 (2H, d, J = 8.8 Hz, ArH-3',5'), 7.16 (1H, d, J = 7.6 Hz, PyH-5), 7.95 (1H, d, J = 7.6 Hz, PyH-4); MS m/z (%) 261 (M–65[–], 100), 325 (M–1[–], 46); HPLC purity 97.4%.

4.27. Ethyl 2-(*N*-(4-methoxyphenyl)-*N*-methyl)amino-6-trifluoromethylnicotinate (8e)

Prepared in a similar manner as for **7d**. Starting with **8d** (163 mg, 0.5 mmol), EtI (153 mg, 1.0 mmol), and K₂CO₃ (138 mg, 1.0 mmol) to produce 156 mg of **8e**, 88% yield, yellow solid, mp 105–106 °C; ¹H NMR δ ppm 1.09 (3H, t, J = 5.6 Hz, CH₃), 3.50 (3H, s, NCH₃), 3.70 (3H, q, J = 7.2 Hz, OCH₂), 3.79 (3H, s, OCH₃), 4.01 (2H, d, J = 5.6 Hz, CH₂), 6.84 (2H, d, J = 9.2 Hz, ArH-2',6'), 7.04 (2H, d, J = 9.2 Hz, ArH-3',5'), 7.06 (1H, d, J = 7.6 Hz, PyH-5), 7.74 (1H, d, J = 7.6 Hz, PyH-4). MS m/z (%) 355.2 (M+1, 28), 309.3 (M–45, 100); HPLC purity 100.0%.

4.28. Isopropyl 2-(*N*-(4-methoxyphenyl)-*N*-methyl)amino-6-trifluoromethylnicotinate (8f)

Prepared in a similar manner as for **7d**. Starting with **8d** (42 mg, 0.13 mmol), *i*-PrI (66 mg, 0.39 mmol), and K₂CO₃ (54 mg, 0.39 mmol) to produce 45 mg of **8f**, 94% yield, pale yellow solid, mp 108–109 °C; ¹H NMR δ ppm 1.04 (6H, d, J = 6.4 Hz, CH₃×2), 3.49 (3H, s, NCH₃), 3.77 (3H, s, OCH₃), 4.59 (1H, m, CH), 6.84 (2H, d, J = 8.8 Hz, ArH-2',6'), 7.04 (2H, d, J = 8.8 Hz, ArH-3',5'), 7.06 (1H, d, J = 7.6 Hz, PyH-5), 7.72 (1H, d, J = 7.6 Hz, PyH-4). MS m/z (%) 369.3 (M+1, 8), 309.3 (M–59, 100); HPLC purity 96.5%.

4.29. *N*-Methyl 2-(*N*-(4-methoxyphenyl)-*N*-methyl)amino-6-trifluoromethyl nicotinamide (8g)

A solution of **8c** (49 mg, 0.14 mmol) in 3 mL of 30% methylamine–MeOH solution was stirred at rt for 4 days. After removal of solvent in vacuo, the crude product was purified with flash column chromatography (gradient eluant: EtOAc/petroleum ether, 0–60%) to provide 35 mg of **8g**, 74% yield, white solid, mp 151–152 °C; ¹H NMR δ ppm 2.51 (3H, d, J = 4.8 Hz, NHCH₃), 3.42 (3H, s, NCH₃), 3.78 (3H, s, OCH₃), 6.00 (1H, br, CONH), 6.84 (2H, d, J = 8.8 Hz, ArH-2',6'), 6.98 (2H, d, J = 8.8 Hz, ArH-3',5'), 7.20 (1H, J = 7.6 Hz, PyH-5), 7.84 (1H, J = 7.6 Hz, PyH-4); MS m/z (%) 340 (M+1, 4), 309 (M–30, 100); HPLC purity 100.0%.

4.30. 3-Hydroxymethyl-*N*-(4-methoxyphenyl)-*N*-methyl-6-trifluoromethylpyridin-2-amine (8h)

Prepared in a similar manner as for **7f**. Starting with **8c** (136 mg, 0.4 mmol) to produce 102 mg of **8h**, 82% yield, yellow oil. ^1H NMR δ ppm 3.38 (3H, s, NCH_3), 3.80 (3H, s, OCH_3), 4.01 (2H, d, $J = 5.6$ Hz, CH_2), 6.84 (2H, d, $J = 9.2$ Hz, ArH-2',6'), 6.96 (2H, d, $J = 9.2$ Hz, ArH-3',5'), 7.26 (1H, d, $J = 7.6$ Hz, PyH-5), 7.80 (1H, d, $J = 7.6$ Hz, PyH-4); MS m/z (%) 312 ($M+1$, 100); HPLC purity 99.1%.

4.31. 3-Methoxymethyl-*N*-(4-methoxyphenyl)-*N*-methyl-6-trifluoromethylpyridine-2-amine (8i)

Prepared in a similar manner as for **7g**. Starting with **8h** (110 mg, 0.35 mmol), MeI (0.06 mL, 1.0 mmol), and NaH (40 mg, 1.0 mmol, 60% oil suspension) to produce 94 mg of **8i**, 82% yield, yellow oil. ^1H NMR δ ppm 3.17 (3H, s, OCH_3), 3.39 (3H, s, NCH_3), 3.72 (2H, s, OCH_2), 3.80 (3H, s, OCH_3), 6.83 (2H, d, $J = 8.8$ Hz, ArH-2',6'), 6.94 (2H, d, $J = 8.8$ Hz, ArH-3',5'), 7.23 (1H, d, $J = 7.6$ Hz, PyH-5), 7.76 (1H, d, $J = 7.6$ Hz, PyH-4). MS m/z (%) 327 ($M+1$, 27), 295 ($M-31$, 100); HPLC purity 99.6%.

4.32. 3-Cyano-*N*-(4-methoxyphenyl)-*N*-methyl-6-trifluoromethylpyridin-2-amine (8j)

The preparation, work-up, and purity are the same as for **8c**. Starting with 3-cyano-*N*-(4-methoxyphenyl)-6-trifluoromethylpyridin-2-amine (**8b**) (586 mg, 2.0 mmol), MeI (0.25 mL, 4.0 mmol), and NaH (160 mg, 60% oil suspension) in 3 mL of DMF at 0 °C with stirring for 1 hour to afford 565 mg of pure **8j**, 92% yield, white solid, mp 83–84 °C; ^1H NMR δ ppm 3.47 (3H, s, NCH_3), 3.84 (3H, s, OCH_3), 6.96 (2H, d, $J = 9.2$ Hz, ArH-2',6'), 6.98 (1H, d, $J = 7.6$ Hz, PyH-5), 7.20 (2H, d, $J = 9.2$ Hz, ArH-3',5'), 7.77 (1H, d, $J = 7.6$ Hz, PyH-4); MS m/z (%) 308 ($M+1$, 100); HPLC purity 97.6%.

4.33. *N*-(4-Methoxyphenyl)-*N*-methyl-3-(1H-tetrazol-5-yl)-6-trifluoromethylpyridin-2-amine (8k)

To a solution of **8j** (417 mg, 1.3 mmol) in toluene (5 mL) was added 4 drops of water, NaN_3 (266 mg, 4.1 mmol), and $\text{Et}_3\text{N}\cdot\text{HCl}$ (562 mg, 4.1 mmol) successively. The mixture was heated at reflux temperature for 36 h. After cooling to rt, the mixture was added to saturated aq. Na_2CO_3 (5 mL) and water (5 mL), and then extracted with petroleum ether three times. The organic phase was washed successively with water and brine, and dried over MgSO_4 . After removal of petroleum ether in vacuo, 176 mg of unreacted **8c** was recovered from the organic phase. The water phase was acidified with aq. HCl (2 N) to pH 2–3, filtered, and dried to give 262 mg of **8k**, 95% yield, yellow solid, mp 225 °C (decomposition); ^1H NMR ($\text{DMSO}-d_6$) δ ppm 3.36 (3H, s, NCH_3), 3.62 (3H, s, OCH_3), 6.63 (2H, d, $J = 8.8$ Hz, ArH-2',6'), 6.82 (2H, d, $J = 8.8$ Hz, ArH-3',5'), 7.47 (1H, d, $J = 7.6$ Hz, PyH-5), 7.96 (1H, d, $J = 7.6$ Hz, PyH-4). MS m/z (%) 349 ($M-1$, 60), 278 ($M-72$, 100); HPLC purity 95.5%.

4.34. *N*-(4-Methoxyphenyl)-*N*-methyl-3-(1-methyl-tetrazol-5-yl)-6-trifluoromethylpyridin-2-amine (8l)

A mixture of **8k** (101 mg, 0.29 mmol), Me_2SO_4 (0.05 mL, 0.58 mmol), and K_2CO_3 (80 mg, 0.58 mmol) in acetone (5 mL) was refluxed for 5 h. After cooling to rt, additional acetone (ca. 10 mL) was added and solid K_2CO_3 was filtered out. After removal of solvent in vacuo, the residue was purified with flash column chromatography (gradient eluant/ EtOAc /petroleum ether, 0–30%) to afford 55 mg of **8l**, 52% yield, pale yellow solid, mp 115–116 °C; ^1H NMR δ ppm 3.51 (3H, s, NCH_3), 3.69 (3H, s, NCH_3),

4.08 (3H, s, OCH_3), 6.60 (2H, d, $J = 9.2$ Hz, ArH-2',6'), 6.83 (2H, d, $J = 9.2$ Hz, ArH-3',5'), 7.21 (1H, d, $J = 7.6$ Hz, PyH-5), 7.83 (1H, d, $J = 7.6$ Hz, PyH-4); MS m/z (%) 365 ($M+1$, 3), 279 ($M-85$, 100); HPLC purity 100.0%.

4.35. Antiproliferative activity assay

Target compounds were assayed by SRB method for cytotoxic activity using the HTCL assay according to procedures described previously.^{18–20} The panel of cell lines included human lung carcinoma (A-549), epidermoid carcinoma of the nasopharynx (KB), P-gp-expressing epidermoid carcinoma of the nasopharynx (KB_{VIN}), and prostate cancer (DU145). The cytotoxic effects of each compound were expressed as GI_{50} values, which represent the molar drug concentrations required to cause 50% tumor cell growth inhibition.

4.36. Tubulin assays

Tubulin assembly was measured by turbidimetry at 350 nm as described previously.²¹ Assay mixtures contained 1.0 mg/mL (10 μM) tubulin and varying compound concentrations were pre-incubated for 15 min at 30 °C without guanosine 5'-triphosphate (GTP). The samples were placed on ice, and 0.4 mM GTP was added. Reaction mixtures were transferred to 0 °C cuvettes, and turbidity development was followed for 20 min at 30 °C following a rapid temperature jump. Compound concentrations that inhibited increase in turbidity by 50% relative to a control sample were determined.

Inhibition of the binding of [^3H]colchicine to tubulin was measured as described previously.²² Incubation of 1.0 μM tubulin with 5.0 μM [^3H]colchicine and 5.0 μM inhibitor was for 10 min at 37 °C, when about 40–60% of maximum colchicine binding occurs in control samples.

5. Molecular modeling studies

All molecular modeling studies were performed with Discovery Studio 3.0 (Accelrys, San Diego, USA). The crystal structures of tubulin in complex with TN16 (PDB: 3HKD) and with DMDA-colchicine (PDB: 1SAO) were downloaded from the RCSB Protein Data Bank (<http://www.rcsb.org/pdb>) for possible use in the modeling study. We selected the structure 3HKD as our modeling system, because of lower binding energy of **6a** with it and matched binding orientation between **6a** and TN16. The CDocker was used to evaluate and predict in silico binding free energy of the inhibitors and automated docking. The protein protocol was prepared by several operations, including standardization of atom names, insertion of missing atoms in residues and removal of alternate conformations, insertion of missing loop regions based on SEQRES data, optimization of short and medium size loop regions with Looper Algorithm, minimization of remaining loop regions, calculation of pK, and protonation of the structure. The receptor model was typed with the CHARMM forcefield. A binding sphere with radius of 9 Å was defined through the native ligand as the binding site for the study. The docking protocol employed total ligand flexibility and the final ligand conformations were determined by the simulated annealing molecular dynamics search method set to a variable number of trial runs. The docked ligands (**6a**, TN16, DMDA-colchicine, and CA-4) were further refined using in situ ligand minimization with the Smart Minimizer algorithm by the standard parameters. The ligand and its surrounding residues within the above defined sphere were allowed to move freely during the minimization, while the outer atoms were frozen. The implicit solvent model

of Generalized Born with Molecular Volume (GBMV) was also used to calculate the binding energies.

Acknowledgements

This investigation was supported by Grants 81120108022 and 30930106 from the Natural Science Foundation of China (NSFC) awarded to Lan Xie and NIH Grant CA17625-32 from the National Cancer Institute awarded to K. H. Lee. This study was also supported in part by the Taiwan Department of Health, China Medical University Hospital Cancer Research Center of Excellence (DOH100-TD-C-111-005).

Supplementary data

Supplementary data associated with this article can be found, in the online version, at <http://dx.doi.org/10.1016/j.bmc.2012.11.047>. These data include MOL files and InChIKeys of the most important compounds described in this article.

References and notes

- Stanton, R. A.; Gernert, K. M.; Nettles, J. H.; Aneja, R. *Med. Res. Rev.* **2011**, *31*, 443.
- Dumontet, C.; Jordan, M. A. *Nat. Rev. Drug Disc.* **2010**, *9*, 790.
- Wang, X. F.; Tian, X. T.; Ohkoshi, E.; Qin, B. J.; Liu, Y. N.; Wu, P. C.; Hour, M. J.; Hung, H. Y.; Huang, R.; Bastow, K. F.; Janzen, W. P.; Jin, J.; Morris-Natschke, S.; Lee, K. H.; Xie, L. *Bioorg. Med. Chem. Lett.* **2012**, *22*, 6224.
- Using the ChemBioDraw Ultra 12.0 software.
- Schmid, S.; Röttgen, M.; Thewalt, U.; Austel, V. *Org. Biomol. Chem.* **2005**, *3*, 3408.
- Frlan, R.; Kikelj, D. *Synthesis* **2006**, *14*, 2271.
- Li, F.; Wang, Q. R.; Ding, Z. B.; Tao, F. G. *Org. Lett.* **2003**, *5*, 2169.
- Qin, B. J.; Jiang, X. K.; Lu, H.; Tian, X. T.; Barbault, F.; Huang, L.; Qian, K.; Chen, C. H.; Huang, R.; Jiang, S.; Lee, K. H.; Xie, L. *J. Med. Chem.* **2010**, *53*, 4906.
- Onnis, V.; Cocco, M. T.; Lilliu, V.; Congiu, C. *Bioorg. Med. Chem.* **2008**, *16*, 2367.
- Cocco, M. T.; Congiu, C.; Onnis, V.; Morelli, M.; Felipo, V.; Cauli, O. *Bioorg. Med. Chem.* **2004**, *12*, 4169.
- He, X. Y.; Zou, P.; Qiu, J.; Hou, L.; Jiang, S.; Liu, S.; Xie, L. *Bioorg. Med. Chem.* **2011**, *19*, 6726.
- Rubinstein, L. V.; Shoemaker, R. H.; Paull, R. M.; Tosini, S.; Skehan, P.; Scudiero, D. A.; Monks, A.; Boyd, M. R. *J. Natl. Cancer Inst.* **1990**, *82*, 1113.
- Walsh, J. S.; Miwa, G. T. *Annu. Rev. Pharmacol. Toxicol.* **2011**, *51*, 145.
- Dorleans, A.; Gigant, B.; Ravelli, R. B. G.; Mailliet, P.; Mikol, V.; Knossow, M. *PNAS* **2009**, *106*, 13775.
- Barbier, P.; Dorleans, A.; Devred, F.; Sanz, L.; Allegro, D.; Alfonso, C.; Knossow, M.; Peyrot, V.; Andreu, J. M. *J. Biol. Chem.* **2010**, *285*, 31672.
- Mason, R. P.; Zhao, D.; Liu, L.; Trawick, L.; Pinney, K. G. *Integr. Biol.* **2011**, *3*, 375.
- Flynn, B. L.; Gill, G. S.; Grobelny, D. W.; Chaplin, J. H.; Paul, D.; Leske, A. F.; Lavranos, T. C.; Chalmers, D. K.; Charman, S. A.; Kostewicz, E.; Shackleford, D. M.; Morizzi, J.; Hamel, E.; Jung, M. K.; Kremmidiotis, G. *J. Med. Chem.* **2011**, *54*, 6014.
- Boyd, M. R. Status of the NCI preclinical antitumor drug discovery screen. In *Cancer: Principles and Practice of Oncology Updates*; J. B. Lippincott: Philadelphia, 1989; pp 1–12.
- Monks, A.; Scudiero, D.; Skehan, P.; Shoemaker, R.; Paull, K.; Vistica, D.; Hose, C.; Langley, J.; Cronise, P.; Vaigro-Woiff, A.; Gray-Goodrich, M.; Campbell, H.; Mayo, J.; Boyd, M. *J. Natl. Cancer Inst.* **1991**, *83*, 757.
- Houghton, P.; Fang, R.; Techatanawat, I.; Stevenon, G.; Hylands, P. J.; Lee, C. C. *Methods* **2007**, *42*, 377.
- Hamel, E. *Cell Biochem. Biophys.* **2003**, *38*, 1.
- Lin, C. M.; Ho, H. H.; Pettit, G. R.; Hamel, E. *Biochemistry* **1989**, *28*, 6984.